Development 139, 2299-2309 (2012) doi:10.1242/dev.078873

Olig2-dependent developmental fate switch of NG2 cells

Xiaoqin Zhu[1,*], Hao Zuo[1,*], Brady J. Maher[1,‡], David R. Serwanski[1], Joseph J. LoTurco[1,2], Q. Richard Lu[3] and Akiko Nishiyama[1,2,§]

SUMMARY

NG2-expressing cells (NG2 cells or polydendrocytes) generate oligodendrocytes throughout the CNS and a subpopulation of protoplasmic astrocytes in the gray matter of the ventral forebrain. The mechanisms that regulate their oligodendrocyte or astrocyte fate and the degree to which they exhibit lineage plasticity in vivo have remained unclear. The basic helix-loop-helix transcription factor Olig2 is required for oligodendrocyte specification and differentiation. We have found that Olig2 expression is spontaneously downregulated in NG2 cells in the normal embryonic ventral forebrain as they differentiate into astrocytes. To further examine the role of Olig2 in NG2 cell fate determination, we used genetic fate mapping of NG2 cells in constitutive and tamoxifen-inducible Olig2 conditional knockout mice in which Olig2 was deleted specifically in NG2 cells. Constitutive deletion of Olig2 in NG2 cells in the neocortex and corpus callosum but not in ventral forebrain caused them to convert their fate into astrocytes, with a concomitant severe reduction in the number of oligodendrocytes and myelin. Deletion of Olig2 in NG2 cells in perinatal mice also resulted in astrocyte generation from neocortical NG2 cells. These observations indicate that the developmental fate of NG2 cells can be switched by altering a single transcription factor Olig2.

KEY WORDS: NG2, Olig2, Oligodendrocyte progenitor, Myelin, Astrocyte, Fate mapping

INTRODUCTION

NG2 cells or polydendrocytes are defined as cells that express the NG2 proteoglycan and the α receptor for platelet-derived growth factor (PDGFRα). They represent a cell population in the developing and mature central nervous system (CNS) that is distinct from neurons, astrocytes, mature oligodendrocytes and resting microglia (Nishiyama, 2007; Nishiyama et al., 2009). They generate oligodendrocytes in vitro (Levine and Stallcup, 1987; Stallcup and Beasley, 1987) and in vivo (Zhu et al., 2008a; Zhu et al., 2008b; Rivers et al., 2008; Dimou et al., 2008; Zhu et al., 2011), and are hence also referred to as oligodendrocyte precursor cells (OPCs). Previously, we have demonstrated that NG2 cells generate not only oligodendrocytes, in addition to a subset of protoplasmic astrocytes in the gray matter of ventral forebrain but not in the dorsal forebrain or white matter (Zhu et al., 2008a). In a subsequent study using inducible NG2 cell fate mapping, we showed that NG2 cells in prenatal but not postnatal ventral forebrain generate astrocytes (Zhu et al., 2011), suggesting the presence of a signal that restricts postnatal and dorsal NG2 cells to the oligodendrocyte lineage and prevents them from becoming astrocytes.

The basic helix-loop-helix transcription factor (bHLH) Olig2 is essential for the specification and maturation of oligodendrocytes in the spinal cord and forebrain (Zhou and Anderson, 2002; Lu et al., 2002; Takebayashi et al., 2002; Muroyama et al., 2005; Yue et al., 2006; Ligon et al., 2006; Maire et al., 2010). Olig2 is expressed in all NG2 cells and in differentiated oligodendrocytes (Kitada and Rowitch, 2006; Ligon et al., 2006). Olig2 is also expressed in some neural progenitor/stem cells in the subventricular zone (SVZ) (Takebayashi et al., 2000; Hack et al., 2005; Menn et al., 2006; Ligon et al., 2006), which are distinct from NG2 cells (Komitova et al., 2009; Platel et al., 2009). Deletion of Olig2 in neural stem cells resulted in increased expression of glial fibrillary acidic protein (GFAP) in astrocytes of the neocortex and loss of myelin (Cai et al., 2007), while NG2 cells appeared to be unaffected. In cultures of neural stem cells, downregulation or cytoplasmic translocation of Olig2 has been shown to cause a switch from an oligodendrocyte to an astrocyte fate (Setoguchi and Kondo, 2004; Fukuda et al., 2004). However, the role of Olig2 in regulating the fate of NG2 cells is not known. In this study, we demonstrate that constitutive or perinatally induced deletion of Olig2 in NG2 cells in the neocortex and corpus callosum causes their fate switch from oligodendrocyte lineage to astrocytes. These observations indicate that NG2 cells retain developmental glial lineage plasticity, and that Olig2 is crucial for their oligodendrocyte fate.

MATERIALS AND METHODS

Generation of constitutive and inducible NG2 cell-specific Olig2 conditional knockout

For constitutive deletion of Olig2 in NG2 cells, NG2creBAC (Zhu et al., 2008a; Zhu et al., 2008b; Cspg4-cre, Jackson Laboratory strain #008533), Z/EG (Novak et al., 2000) and Olig2 conditional knockout mice (Olig2$^{fl/fl}$ or Olig2$^{fl/+}$) were bred to create homozygous NG2creBAC:ZEG:Olig2$^{fl/fl}$ (Cko) and heterozygous NG2creBAC:ZEG:Olig2$^{fl/+}$ (Ctr) triple transgenic mice. Only female NG2creBAC mice were used for breeding, as the NG2cre transgene is spuriously activated by an unknown mechanism in male germ cells in NG2creBAC mice.

For inducible deletion of Olig2 in NG2 cells, we used mice that were triple transgenic for NG2creER (Zhu et al., 2011) (Cspg4-creER, Jackson Laboratory strain #008538), gtROSA-EYFP (YFP) (Srinivas et al., 2001) (Jackson Laboratory strain #006148), and Olig2$^{fl/fl}$ (iCko) or Olig2$^{fl/+}$(iCtr), and Cre was induced by intraperitoneal injection of 0.2 mg of 4-hydroxytamoxifen (4OHT; Sigma) once daily for four consecutive days, as previously described (Zhu et al., 2011). All animal procedures were approved by the Institutional Animal Care and Use Committee.

[1]Department of Physiology and Neurobiology, University of Connecticut, 75 North Eagleville Road, Storrs, CT 06269-3156, USA. [2]Stem Cell Institute and Center for Regenerative Biology, Storrs, CT 06269, USA. [3]University of Texas Southwestern Medical Center, Department of Developmental Biology and Kent Waldrep Foundation Center for Basic Neuroscience Research on Nerve Growth and Regeneration, Dallas, TX 75390, USA.

*These authors contributed equally to this work
‡Present address: Lieber Institute for Brain Development, Johns Hopkins Medical Campus, Baltimore, MD 21205, USA
§Author for correspondence (akiko.nishiyama@uconn.edu)

Accepted 25 April 2012

Tissue processing and immunohistochemistry

Tissue sections were prepared and processed for immunohistochemistry as previously described (Zhu et al., 2008a; Zhu et al., 2011). The source and dilution of the primary antibodies used are listed in supplementary material Table S1. For Ki-67 immunolabeling, antigen retrieval was performed as described by Jiao et al. (Jiao et al., 1999) on 20 μm cryostat sections from fixed frozen tissue.

Cell counts

Cell counts were obtained in 50 μm coronal sections through the cerebrum at the level of the anterior commissure or transverse spinal cord sections from P4, P12 and P21 Cko and Ctr mice. Using a 20× or 40× objective lens, the optical fields were randomly selected and scanned in the neocortex, corpus callosum, ventral forebrain or spinal cord, and z-stack images were acquired using a Zeiss Axiovert 200M equipped with Hamamatsu ORCA ER camera and Apotome or Leica TCS SP2 confocal laser scanning microscope. Area measurements were obtained using the AxioVision or Leica confocal software. Quantification was performed similarly for NG2creER:YFP:Olig2$^{fl/fl}$ (iCko) and NG2creER:YFP:Olig^{fl+} (iCtr) mice. YFP was detected with an antibody to GFP.

The total number of EGFP-negative resident astrocytes was estimated at P4, P12 and P21 by first obtaining the density of astrocytes in the neocortex in 4-5 randomly chosen fields of a defined area. The volume of the neocortex in each section was obtained by multiplying the area by the thickness of the section (50 μm) and was used to calculate the total number of EGFP-negative astrocytes in the section. The results of quantification are expressed as averages ± s.d.

Electron microscopy

P21 Cko and Ctr mice were anesthetized and perfused with 2% paraformaldehyde and 2.5% glutaraldehyde in 0.1 M cacodylate buffer (pH 7.4). Isolated brains were postfixed in the same fixative for 1 hour on ice, rinsed in cold 0.1 M cacodylate buffer and postfixed in 1% OsO_4 in cacodylate for 1 hour at room temperature. They were then rinsed in distilled H_2O and dehydrated in an ascending series of ethanol followed by treatment in propylene oxide. Tissues were infiltrated in a 1:1 and 1:3 catalyzed mixture of propylene oxide to resin (Embed 812) for 2 hours each, followed by an overnight infiltration in 100% resin and embedded the next day in newly prepared resin and polymerized at 60°C for 48 hours. Ultrathin (70 nm) sections were cut on a Leica Ultracut microtome, placed on 200 mesh copper grids and counterstained with 2% aqueous uranyl acetate and Sato's lead citrate for 5 and 3 minutes, respectively. Digital images were acquired using a FEI Technai Biotwin electron microscope.

Electrophysiology

Mice were anesthetized with isoflurane and decapitated. Brains were immersed in ice-cold oxygenated (95% O_2, 5% CO_2) dissection buffer containing (in mM): 83 NaCl, 2.5 KCl, 1 NaH_2PO_4, 26 $NaHCO_3$, 22 glucose, 72 sucrose, 0.5 $CaCl_2$ and 3.3 $MgCl_2$. Coronal brain slices were prepared from P19-21 Cko and Ctr mice using a Vibratome (VT1000S; Leica), incubated in dissection buffer for 30-45 minutes at 37°C and then stored at room temperature. Slices were visualized using infrared differential interference contrast microscopy (Nikon E600FN) and a CCD camera (QImaging). EGFP$^+$ NG2 cells were visualized with epifluorescence illumination and a 40× Nikon water-immersion lens (numerical aperture 0.8).

For all experiments, artificial cerebrospinal fluid was oxygenated (95% O_2, 5% CO_2) and contained (in mM); 125 NaCl, 25 $NaHCO_3$, 1.25 NaH_2PO_4, 3 KCl, 25 glucose, 2 $CaCl_2$ and 1 $MgCl_2$ (pH 7.3). Patch pipettes were fabricated from borosilicate glass to resistance of 4-6 MΩ. Pipettes were filled with (in mM): 125 potassium gluconate, 10 Hepes, 4 Mg-ATP, 0.3 Na-GTP, 0.1 EGTA, 10 phosphocreatine and 0.05% biocytin, and adjusted to pH 7.3 with KOH. Current signals recorded with a Multiclamp 700A amplifier (Molecular Devices) were filtered at 2 kHz using a built-in Bessel filter and digitized at 10 kHz. Data were acquired using Axograph.

Recorded cells were injected with biocytin. After completion of the recording, slices were fixed in 4% paraformaldehyde for 1 hour, followed by rinses in 0.2 M sodium phosphate buffer (pH 7.4) and blocked and permeabilized in 5% normal goat serum and 0.1% Triton X-100. Biocytin was visualized with Cy3-conjugated streptavidin (Jackson ImmunoResearch, 1:200 dilution). Aldh1L1, GFAP and NG2 were detected by immunohistochemistry.

RESULTS

Olig2 is expressed in NG2 cells but not in NG2 cell-derived astrocytes

Previously, we reported that NG2 cells in the embryonic ventral forebrain generate a subset of protoplasmic astrocytes in addition to oligodendrocytes (Zhu et al., 2008a; Zhu et al., 2011) and identified transitional cells in the ventral forebrain of embryonic day (E) 18.5 NG2creBAC:ZEG double transgenic mice (Zhu et al., 2008a). We examined the expression of the oligodendrocyte bHLH transcription factor Olig2 in EGFP$^+$ progeny of NG2 cells (Fig. 1). At postnatal day 14 (P14), robust nuclear Olig2 immunoreactivity was detected in the majority of EGFP$^+$ cells with the characteristic morphology of polydendrocytes or oligodendrocytes in the neocortex, corpus callosum and ventral forebrain (Fig. 1A-C). By contrast, Olig2 was absent in EGFP$^+$ protoplasmic astrocytes (Fig. 1C, arrowheads). In the ventral forebrain of E18.5 NG2creBAC:ZEG brain where transitional forms were found, EGFP$^+$ cells with little detectable NG2 had weaker Olig2 immunoreactivity (arrowheads in Fig. 1E), while EGFP$^+$ cells with strong NG2 immunoreactivity typical of polydendrocytes exhibited stronger nuclear Olig2 immunoreactivity (arrows in Fig. 1D,E). These observations suggest that Olig2 is spontaneously lost as NG2 cells in the ventral forebrain differentiate into protoplasmic astrocytes.

Deletion of Olig2 in NG2 cells in NG2creBAC:ZEG:Olig2$^{fl/fl}$ (Cko) mice

To examine the role of Olig2 in regulating the fate of NG2 cells, the phenotype of EGFP$^+$ progeny of NG2 cells was analyzed in mice that were triple transgenic for Olig2$^{fl/fl}$ (Yue et al., 2006), NG2creBAC and Z/EG (NG2creBAC:ZEG:Olig2$^{fl/fl}$ mice, conditional knockout; Cko). Littermate mice that were heterozygous for the floxed Olig2 allele (NG2creBAC:ZEG:Olig2$^{fl/+}$) were used as controls (Ctr). Previous studies showed no discernible phenotype in heterozygous Olig2 knockout mice (Yue et al., 2006; Cai et al., 2007).

To assess the extent of Olig2 deletion, the percentage of Olig2$^-$ cells among EGFP$^+$ cells was determined in different regions of P21 Cko and Ctr brain (Table 1, first column). Although the majority of EGFP$^+$ cells in the Ctr brain were Olig2$^+$ (supplementary material Fig. S1B,D,F), fewer than 1% of EGFP$^+$ cells in the neocortex, corpus callosum and the ventral cortex (entorhinal cortex) had detectable Olig2 (Table 1; supplementary material Fig. S1A,C,E). In the cingulate cortex of Cko mice, a greater proportion of EGFP$^+$ cells (2.3%) expressed Olig2 (supplementary material Fig. S1G; Table 1), which is likely to have been caused by a lower efficiency of Cre-mediated recombination among NG2 cells in this region.

Loss of Olig2 converts NG2 cells in the dorsal forebrain into astrocytes

NG2 cells are converted into protoplasmic astrocytes in the neocortex of Olig2 Cko mice

In the neocortex of P21 Cko mice, the majority of EGFP$^+$ cells had highly branched bushy processes characteristic of protoplasmic astrocytes (Fig. 2A; supplementary material Fig. S1A) (Bushong et al., 2002), in contrast to the typical polydendrocyte morphology of

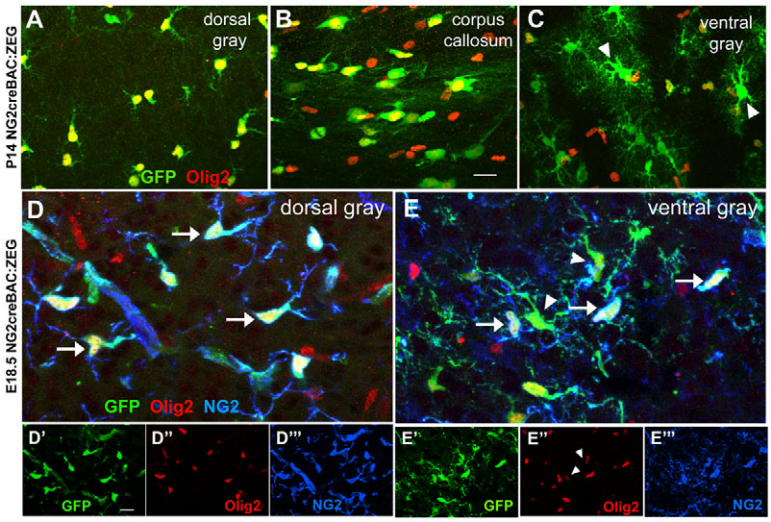

Fig. 1. Expression of Olig2 in NG2 cells but not in NG2 cell-derived astrocytes. (**A-C**) Coronal sections from the neocortex (A), corps callosum (B) and ventral forebrain gray matter (C) of P14 NG2creBAC:ZEG double transgenic mice immunolabeled for Olig2 (red). Green represents EGFP fluorescence. Olig2 is present in EGFP⁺ cells with the morphology of NG2 cells and oligodendrocytes in the neocortex and corpus callosum, but not in EGFP⁺ astrocytes (arrowheads) in the ventral forebrain. (**D-E″**) Coronal sections from the neocortex and ventral forebrain of E18.5 NG2creBAC:ZEG double transgenic mice double immunolabeled for Olig2 (red) and NG2 (blue). Green represents EGFP fluorescence. Images from each color channel are shown below the merged images. Olig2 is more robustly expressed in EGFP⁺ cells with strong NG2 immunoreactivity and typical polydendrocyte morphology (arrows in D,E) than in EGFP⁺ cells in the ventral forebrain with multiple processes and weak NG2 immunoreactivity (arrowheads in E,E″). Scale bars: 20 μm.

EGFP⁺ cells in the Ctr cortex (Fig. 2B,D; supplementary material Fig. S1B). EGFP⁺ astrocytes in Cko cortex were arranged in broad patches that occupied a large area of the cortex, and their density correlated with the extent of Olig2 deletion. NG2⁺ cells were almost completely absent in areas where Olig2 had been successfully deleted, and the only NG2-immunoreactive structures were the vasculature (Fig. 2C). As discussed below, the loss of NG2⁺ cells is probably due to conversion of existing NG2 cells into astrocytes and not due to compromised survival of NG2 cells. EGFP⁺ bushy cells in the neocortex of Cko mice expressed the astrocytic antigen aldehyde dehydrogenase 1 L1 (Aldh1L1) (Cahoy et al., 2008) (Fig. 2E) as well as S100β (not shown). The level of GFAP was elevated in EGFP⁺ astrocytes in the neocortex of Cko mice compared with that in Ctr mice (supplementary material Fig. S2A,B). EGFP⁺ astrocytes comprised 70.3±6.9% of the entire Aldh1L1⁺ astrocyte population in Cko neocortex at P21, whereas none of the astrocytes in Ctr neocortex expressed EGFP (Fig. 3). In the cingulate cortex of Cko mice, there was a small number of EGFP⁻ NG2⁺ Olig2⁺ cells (supplementary material Fig. S1G; Table 1, last column), suggesting that NG2 cells in this region that had not undergone Cre-mediated excision of Olig2 did not differentiate into astrocytes.

EGFP⁺ astrocytes in the corpus callosum of Olig2 Cko mice

In the corpus callosum of P21 Cko mice, some EGFP⁺ cells exhibited astrocytic morphology with multiple spiny bushy processes (arrow in supplementary material Fig. S2C) and were distinct from EGFP⁺ oligodendrocytes with large oval cell bodies and thick smooth processes seen in Ctr mice (supplementary material Fig. S2D). By contrast, EGFP⁺ NG2⁺ cells had fewer long slender processes and were negative for Aldh1L1, similar to those seen in Ctr corpus callosum (arrowheads in supplementary material Fig. S2C). EGFP⁺ astrocytes represented 20.0±6.7% of the total Aldh1L1⁺ astrocyte population in the corpus callosum (Fig. 3). In Ctr mice, EGFP⁺ cells were either oligodendrocytes or NG2 cells and were never Aldh1L1⁺ (Fig. 3).

No increase in EGFP⁺ astrocytes in the ventral forebrain and spinal cord of Olig2 Cko mice

In the gray matter of the ventral forebrain, where we previously observed that NG2 cells generate more than one-third of the S100β⁺ astrocytes during normal development (Zhu et al., 2008a; Zhu et al., 2011), many EGFP⁺ cells with protoplasmic astrocytic morphology were found (arrows in supplementary material Fig. S2E) in P21 Olig2 Cko mice, intermingled with EGFP⁺ NG2⁺ cells with typical polydendrocyte morphology (arrowheads in supplementary material Fig. S2E). However, the proportion of Aldh1l1⁺ astrocytes that were EGFP⁺ in the ventral forebrain of Cko mice was slightly higher but not statistically different from that in Ctr mice (Fig. 3). Thus, deletion of Olig2 in NG2 cells did not result in a significant conversion of NG2 cells into astrocytes in regions where NG2 cells in the embryonic brain normally generate a subpopulation of astrocytes after spontaneously downregulating Olig2 expression (Zhu et al., 2008a; Zhu et al., 2011). Consistent with this, the density of NG2⁺ cells was higher in the ventral forebrain, despite successful deletion of Olig2, than in the dorsal forebrain (Table 1; supplementary material Fig. S1E). Thus, in the ventral forebrain, Olig2-deleted NG2 cells remained in the oligodendrocyte. The regional differences in the fate of NG2 cells in normal and Olig2-deleted conditions are schematically shown in the lineage diagram in Fig. 9 (see Discussion below). In the spinal cord of P21 Olig2 Cko mice, 1.6±1.66% and 1.3±0.61% of EGFP⁺ cells were Aldh1l1⁺ in the ventral and dorsal gray matter, respectively, whereas in P21 Ctr spinal cord, 0.4±0.33% and

Table 1. Efficiency of Olig2 deletion in P21 Cko brain

		Density/mm²		
	%Olig2⁺/EGFP⁺	EGFP⁺	Olig2⁺*	NG2⁺*
Dorsal cortex	0.5±0.45	181.1±31.62	24.7±19.93	10.0±6.20
Ventral cortex	0.6±0.51	202.2±36.72	8.2±3.23	87.4±13.08
Cingulate cortex	2.3±2.27	191.8±53.03	33.2±12.91	43.3±17.43
Corpus callosum	0.0±0.00	275.4±33.90	34.0±8.81	96.8±17.20

*Most were EGFP negative.

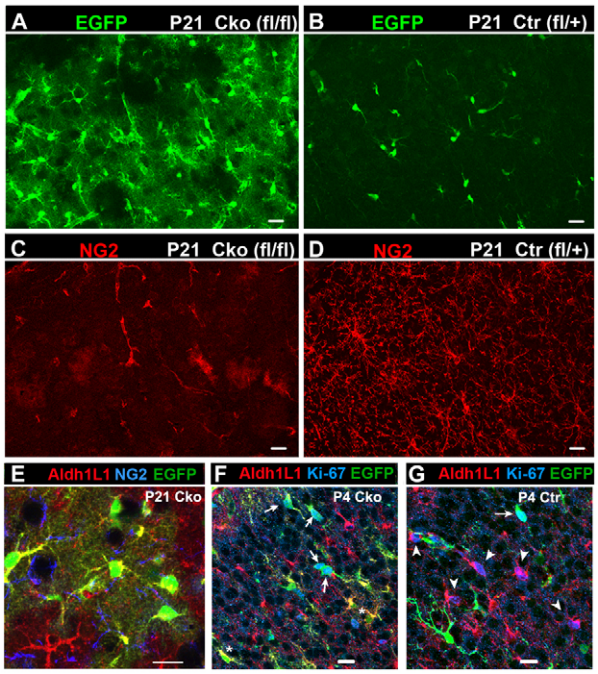

Fig. 2. NG2 cell-derived astrocytes in the dorsal forebrain of P21 Olig2 Cko and Ctr mice. (**A-D**) EGFP fluorescence (green, A,B) and NG2 immunolabeling (red, C and D) of the neocortex of P21 Olig2 Cko (A,C) and Ctr (B,D) mice. Upper left is pial surface. NG2$^+$ EGFP$^+$ polydendrocytes in the Ctr cortex are completely replaced by NG2-negative EGFP$^+$ protoplasmic astrocytes in Cko brain, where NG2 immunoreactivity is detected only in the vasculature (C). (**E**) Coronal section through P21 Cko neocortex stained for Aldh1L1 (red) and NG2 (blue). EGFP$^+$ NG2 cell-derived protoplasmic astrocytes are Aldh1L1$^+$. (**F**,**G**) EGFP fluorescence (green) and immunolabeling for Aldh1L1 (red) and Ki-67 (blue) in the neocortex of Cko (F) and Ctr (G) mice at P4. In Cko neocortex, Ki-67 is detected mostly in EGFP$^+$ cells (arrows in F) but rarely in EGFP$^-$ Aldh1L1$^+$ cells, and some EGFP$^+$ cells express Aldh1L1 (asterisk in F). In Ctr mice, many EGFP$^-$ Aldh1L1$^+$ resident astrocytes are Ki-67$^+$ (arrowheads in G). Occasional EGFP$^+$ Ki-67$^+$ cells are seen in Ctr (arrow in G). Scale bars: 20 μm.

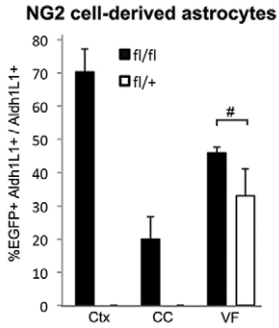

Fig. 3. Astrocyte differentiation from NG2 cells in different regions. Percentages of NG2 cell-derived astrocytes (EGFP$^+$ Aldh1l1$^+$) among total Aldh1L1$^+$ astrocytes in the neocortex (Ctx), corpus callosum (CC) and gray matter of the ventral forebrain (VF) in Cko (fl/fl, filled bars) and Ctr (fl/$^+$, open bars) mice at P21. Error bars indicate s.d. In the ventral forebrain, there was no significant difference (P=0.055, n=3, Student's t-test, bracket with #) in the percentage of astrocytes that were EGFP$^+$ in Cko and Ctr mice (45±1.7% and 33±8.0%, respectively). No EGFP$^+$ Aldh1L1$^+$ astrocytes were detected in the neocortex or corpus callosum of Ctr mice.

0.8±0.17% of EGFP$^+$ cells were Aldh1L1$^+$ in the ventral and dorsal gray matter, respectively. EGFP$^+$ Aldh1L1$^+$ astrocytes were not detected in the white matter of the spinal cord.

Severe reduction of oligodendrocytes and myelin in the dorsal forebrain of Olig2 Cko mice

In the neocortex of P21 Cko mice where NG2 cell-derived astrocytes were most abundant, the number of oligodendrocytes identified by immunoreactivity for glutathione S-transferase π (GST-π) was dramatically reduced and was completely devoid in some areas (Fig. 4A). GST-π was used to identify oligodendrocytes in the neocortex rather than the CC1 monoclonal antibody that is commonly used in the white matter because the CC1 antibody recognizes astrocytes in addition to oligodendrocytes in gray matter. The few GST-π$^+$ oligodendrocytes that were present lacked EGFP (Fig. 4C), suggesting that NG2 cells that had escaped Cre-mediated recombination and retained Olig2 had differentiated into oligodendrocytes. By contrast, in the neocortex of P21 Ctr mice, there were numerous EGFP$^+$ GST-π$^+$ oligodendrocytes (Fig. 3B,D).

In the corpus callosum of P21 Cko mice, the density of CC1$^+$ oligodendrocytes was ~50% of that in Ctr corpus callosum (Fig. 4E,F, Fig. 5). The majority of CC1$^+$ oligodendrocytes in Cko corpus callosum were EGFP negative (Fig. 4G), suggesting that NG2 cells that escaped Olig2 deletion differentiated into oligodendrocytes, as in the neocortex. Immunoreactivity for myelin basic protein (MBP) was severely reduced in the corpus callosum of P21 Cko mice, especially in its lateral aspects (Fig. 4I,J). A few strands of MBP$^+$ fibers were seen in the corpus callosum near the midline, where Olig2 immunoreactivity persisted, suggesting that some myelinating oligodendrocytes had been generated from NG2 cells that had escaped Olig2 deletion. Ultrastructural analysis also showed an almost complete absence of myelin around axons in the corpus callosum of P21 Cko mice (supplementary material Fig. S3).

Functional characterization of NG2 cell-derived astrocytes in Olig2 Cko mice

To examine the functional properties of NG2 cell-derived protoplasmic astrocytes in Olig2 Cko brain, we compared the membrane properties of EGFP$^+$ cells in neocortical slices from P19-21 Cko and Ctr mice. EGFP$^+$ cells in the Cko cortex had a resting membrane potential of –82.3±1.8 mV and an input resistance of 19.8±2.5 MΩ (n=10), typical of passive astrocytes (Steinhauser et al., 1994; Lin and Bergles, 2002). By contrast, EGFP$^+$ cells from Ctr neocortex displayed a more depolarized resting membrane potential [–76.5±0.5mV (n=4); P<0.015] and a mean input resistance of 330.4±219.6 MΩ (n=4), typical of NG2 cells (Lin and Bergles, 2002). Voltage-steps and ramp protocols in EGFP$^+$ cells from Cko neocortex showed linear current-voltage relationships (supplementary material Fig. S4Aa,b), similar to those reported for passive astrocytes (Zhou et al., 2006). By contrast, EGFP$^+$ cells from Ctr neocortex displayed non-linear current-voltage relationships with pronounced outward rectification (supplementary material Fig. S4Ba,b), commonly observed in NG2 cells or previously reported 'complex cells' (Steinhauser et al., 1994; Lin and Bergles, 2002). Immunohistochemistry of biotin-filled recorded cells confirmed that the recorded cells in the Cko cortex were Aldh1L1$^+$ and GFAP$^+$ (supplementary material Fig.S4Ac,d), whereas those in the Ctr cortex were NG2$^+$ (supplementary

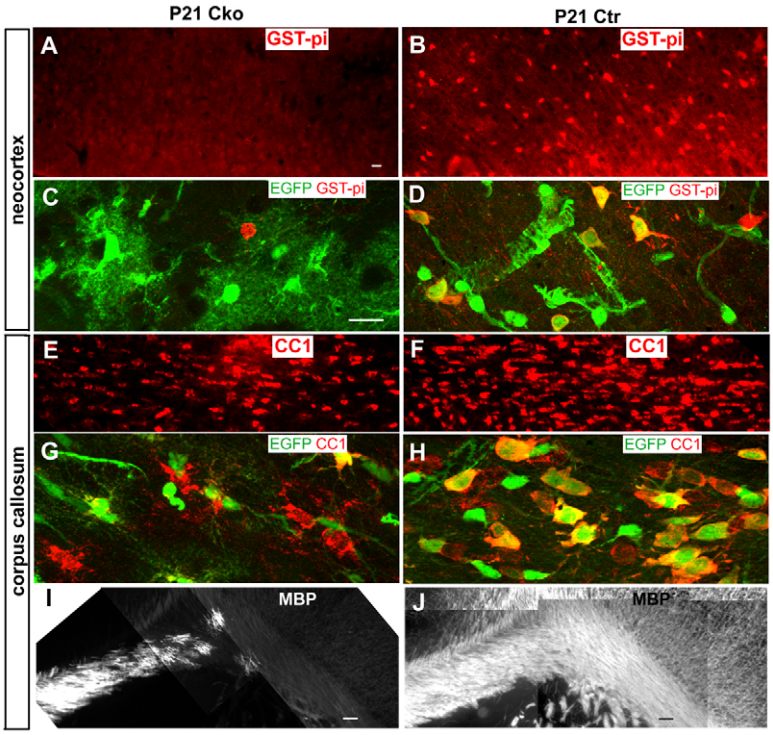

Fig. 4. Oligodendrocyte and myelin defects in P21 Cko brain. (**A-D**) Coronal sections through the neocortex of Cko (A,C) and Ctr (B,D) labeled for GST-π (red) showing an almost complete absence of oligodendrocytes in Cko neocortex. Higher magnification images show the presence of one EGFP⁻ GST-π⁺ oligodendrocyte in the neocortex of Cko mice (C), in contrast to the numerous EGFP⁺ GST-π⁺ oligodendrocytes in Ctr neocortex (D). (**E-H**) Coronal sections through the corpus callosum of Cko (E,G) and Ctr (F,H) mice labeled with the CC1 antibody (red). There are fewer CC1⁺ oligodendrocytes in Cko corpus callosum (E), where the majority of CC1⁺ oligodendrocytes are EGFP⁻ (G). (**I**,**J**) Coronal sections through the corpus callosum immunolabeled for MBP. Left is medial. In Cko, a small amount of myelin is detected in the medial forebrain, but myelin is almost completely absent in the more lateral regions. Scale bars: 20 μm.

material Fig. S4Bc). These findings suggest that downregulation of Olig2 expression drives NG2 cells to biophysically and morphologically resemble passive astrocytes.

NG2 cells develop into astrocytes after birth in the neocortex of Olig2 Cko mice

We next examined when NG2 cells in the neocortex of Olig2 Cko mice were transformed into astrocytes. At P0, EGFP⁺ cells expressed NG2 and had the morphology of typical polydendrocytes (Fig. 6A), similar to the EGFP⁺ cells in P0 Ctr neocortex (Fig. 6B), and EGFP⁺ NG2⁻ cells were not found. By P4, some EGFP⁺ cells in the neocortex of Cko mice had a more highly branched bushy morphology, intermediate between NG2 cells and mature bushy protoplasmic astrocytes (Fig. 6C, arrow). These intermediate EGFP⁺ cells had weak immunoreactivity for NG2 and PDGFRα (Fig. 6C,E, arrows), especially in the distal processes, whereas their cell bodies contained Aldh1L1 (Fig. 6C, inset; 6E, asterisks), in contrast to the typical NG2 cells that had fewer slender processes and strong immunoreactivity for NG2 or PDGFRα (Fig. 6C,E, arrowheads). Some EGFP⁺ Aldh1L1⁺ cells also expressed the oligodendrocyte lineage transcription factor Sox10 (Fig. 6F, asterisks). In the neocortex of P4 Ctr mice, we did not detect any EGFP⁺ cells with bushy processes or Aldh1L1 expression, and the non-vascular EGFP⁺ cells were NG2⁺ cells with the typical polydendrocyte morphology (Fig. 6D).

Deletion of Olig2 in postnatal NG2 cells also causes astrocyte differentiation

The experiments described above were performed using NG2creBAC mice that expressed Cre constitutively in NG2 cells after embryonic day 16, which marks the first appearance of NG2 protein in CNS parenchyma outside the vasculature (Zhu et al., 2008a). To determine whether deletion of Olig2 from NG2 cells in older mice could also cause their fate switch, Olig2 was deleted perinatally by injecting 4OHT between P2 and P5 in mice that were triple transgenic for NG2creER, ROSA-EYFP reporter (YFP) and Olig2$^{fl/fl}$ (iCko) or Olig2$^{fl/+}$ (iCtr). The percentage of Olig2-negative YFP⁺ cells that expressed the astrocyte antigen glutamine synthetase (GS) and had bushy morphology was obtained 14 and 30 days after Cre induction (14 and 30 dpi). GS was used instead of Aldh1L1 because it was more readily detectable in protoplasmic astrocytes in older brains than Aldh1L1. Olig2 deletion at P2-5 resulted in a gradual increase in the number of YFP⁺ astrocytes in the neocortex of iCko mice from 23% of YFP⁺ Olig2⁻ cells at 14 dpi to 55% at 30 dpi (Fig. 7A, arrowheads; 7C). The remaining YFP⁺ cells in Cko cortex had the typical morphology of polydendrocytes (Fig. 7A, arrow). By contrast, all the YFP⁺ cells in Ctr neocortex expressed Olig2 and had the typical polydendrocyte morphology (arrows in Fig. 7B). None of the YFP⁺ cells in the Ctr brain expressed Aldh1L1 at 14 or 30 dpi. These

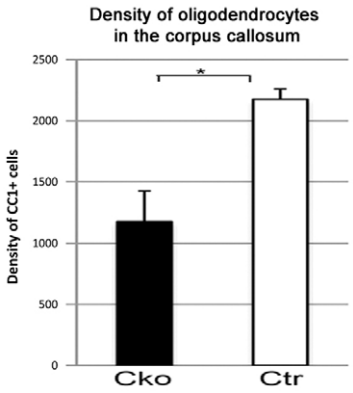

Fig. 5. Decreased oligodendrocyte generation in Cko corpus callosum. The density of CC1⁺ oligodendrocytes (numbers of CC1⁺ cells/mm^2) in the corpus callosum of Cko (filled bars) is significantly reduced compared with that in Ctr (open bars). *P<0.05, Student's t-test. Data are mean±s.d.

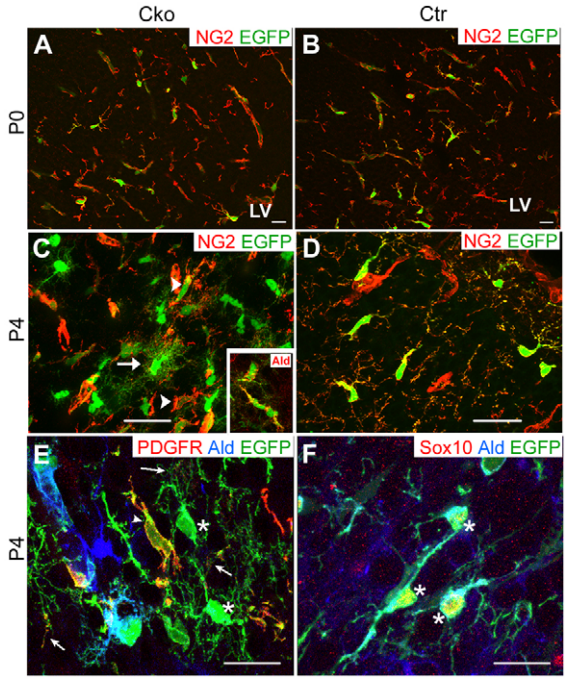

Fig. 6. The transition from NG2 cells to astrocytes in early postnatal Olig2 Cko brain. (**A**,**B**) Coronal sections through the neocortex of P0 Cko (A) and Ctr (B) mice immunolabeled for NG2 (red). All the EGFP$^+$ cells (green) are NG2$^+$. (**C**,**D**) Coronal sections through the neocortex of P4 Cko (C) and Ctr (D) mice immunolabeled for NG2 (red). Some EGFP$^+$ cells express weak or little NG2 (e.g. cell with arrow in C) compared with the strong NG2 immunoreactivity in polydendrocytes (arrowhead in C and EGFP$^+$ cells in D). Inset in C shows Aldh1L1 immunolabeling (Ald) in Cko neocortex. Some of the EGFP$^+$ cells express Aldh1L1. (**E**) Coronal section through the neocortex of P4 Cko mouse immunolabeled for PDGFRα (red) and Aldh1L1 (blue). Arrowhead shows a typical EGFP$^+$ polydendrocyte with strong PDGFRα immunoreactivity. Asterisks show EGFP$^+$ cell bodies with faint Aldh1L1 immunoreactivity in their somata and faint PDGFRα immunoreactivity in their distal processes (arrows), indicative of transitional cells that are losing PDGFRα and acquiring Aldh1L1. (**F**) Coronal section through P4 Cko neocortex immunolabeled for Sox10 (red) and Aldh1L1 (blue). Asterisks show a cluster of three EGFP$^+$ Sox10$^+$ and Aldh1L1$^+$ cells. Scale bars: 20 μm.

observations suggest that NG2 cells retain the ability to generate astrocytes upon Olig2 deletion after birth, although the fate switch from perinatal NG2 cells is incomplete and occurs over a more protracted period of time compared with embryonic NG2 cells.

Expansion of normal resident astrocytes is repressed in Olig2 Cko neocortex

During normal development, astrocytes are generated from radial glial cells (Voigt, 1989; Gray and Sanes, 1992; Malatesta et al., 2000), the SVZ (Levison and Goldman, 1993; Zerlin et al., 2004; Ganat et al., 2006) and possibly from astrocyte precursors that exist in the parenchyma (Pringle et al., 2003; Zawadzka et al., 2010). As a substantial number of NG2 cell-derived astrocytes were generated in Olig2 Cko mice in addition to the astrocytes that arose from the normal sources, we examined whether the astrocyte population was expanded in Olig2 Cko mice. Contrary to our expectations, the density of astrocytes in all the three brain regions of Cko mice was not higher than that in Ctr mice (Fig. 8A). The number of EGFP-negative astrocytes that presumably arose from normal sources in Ctr neocortex expanded between P4 and P21, whereas the number of EGFP-negative astrocytes in Cko neocortex did not change between P4 and P12 and declined by P21 (Fig. 8B). The proportion of Ki-67$^+$ EGFP$^-$ Aldh1L1$^+$ cells among total EGFP$^-$ Aldh1L1$^+$ cells in P4 Ctr neocortex, which represented proliferating resident astrocytes, was 7.1±0.52%, whereas that in Cko neocortex was dramatically lower at 0.95±0.63% (Fig. 2F,G). In Cko cortex, the majority of Ki-67$^+$ proliferating cells were EGFP$^+$ Aldh1L1$^-$ NG2 cells (arrows in Fig. 2F). After P4, very few Ki-67$^+$ astrocytes were detected in Ctr and Cko cortex. These observations suggest that in Cko neocortex, a homeostatic feedback mechanism inhibits proliferation of normal resident astrocytes as more astrocytes are generated from NG2 cells, leading to preservation of the normal density of astrocytes.

DISCUSSION

Specific deletion of Olig2 in NG2 cells

Olig2 is expressed in all NG2 cells (Ligon et al., 2006; Kitada and Rowitch, 2006), which are further committed toward the oligodendrocyte lineage than neural stem cells. Although the loss of Olig2 from the nucleus of neural stem cells has been shown to promote astrocyte differentiation and inhibit oligodendrocyte differentiation (Fukuda et al., 2004; Kondo and Raff, 2004; Setoguchi and Kondo, 2004), the role of Olig2 in regulating NG2 cell fate had not been explored. Our observation that, during normal development, Olig2 expression is spontaneously downregulated in NG2 cells that appear to be transforming into astrocytes in the embryonic ventral forebrain (Fig. 1), suggests that ultimately the loss of Olig2 is required for NG2 cells to follow an astrocytic fate. It remains unknown whether the observed loss of Olig2 is a consequence of an altered phosphorylation status (Li et al., 2011). Neither is it known why some NG2 cells in the ventral forebrain spontaneously downregulate Olig2 expression and become astrocytes whereas those in the dorsal forebrain and white matter remain in the oligodendrocyte lineage.

To determine whether genetic deletion of Olig2 can further convert NG2 cells into astrocytes, we examined the fate of NG2 cells in Olig2 Cko mice. In the forebrain of Olig2 Cko mice, Olig2 was successfully deleted in >99% of EGFP$^+$ cells in the neocortex, corpus callosum and ventral forebrain, such as the entorhinal cortex, with a similar efficiency of Cre excision (%EGFP$^+$ among NG2$^+$ cells) to that previously described for NG2creBAC:ZEG mice (Zhu et al., 2008a). Olig2 deletion was less complete in medial forebrain structures such as the cingulate cortex and midline corpus callosum. Some Olig2$^+$ cells that were NG2 negative were found primarily in the SVZ, suggesting that they were NG2-negative type B or type C neural progenitor cells (Menn et al., 2006; Hack et al., 2005; Komitova et al., 2009; Platel et al., 2009).

Fate switch of neocortical NG2 cells into astrocytes upon Olig2 deletion

The most dramatic effect was seen in the neocortex, where Olig2-deleted NG2 cells became protoplasmic astrocytes that were morphologically, immunohistochemically and electrophysiologically indistinguishable from normal resident protoplasmic astrocytes. Astrocyte differentiation from NG2 cells occurred at the expense of oligodendrocytes, resulting in severe depletion of oligodendrocytes and hypomyelination. This is partially corrected by P60 owing to increased proliferation and differentiation of non-recombined EGFP-negative Olig2$^+$ NG2 cells (data not shown).

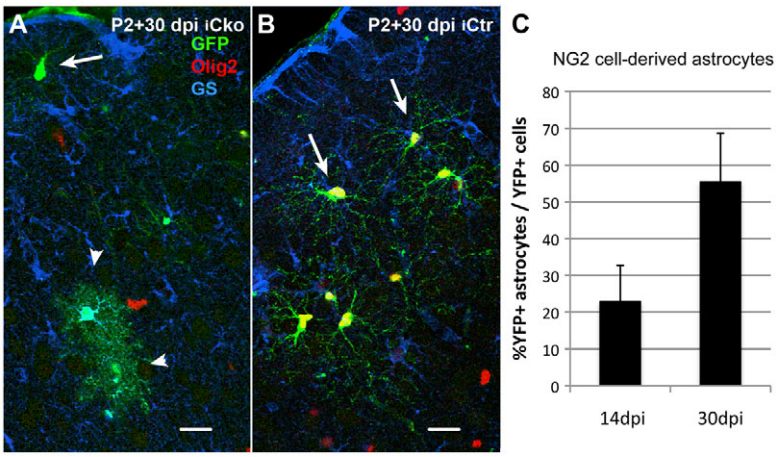

Fig. 7. Astrocyte differentiation from postnatal NG2 cells in Olig2 iCko neocortex. (**A**,**B**) Triple labeling for GFP (green), Olig2 (red) and GS (blue) in the neocortex of NG2creER:YFP:Olig2$^{fl/fl}$ (iCko, A) and NG2creER:YFP:Olig2$^{fl/+}$ (iCtr, B) mice 30 days after Cre induction at P2-5. Arrowheads in A indicate YFP$^+$ GS$^+$ astrocytes that are the progeny of NG2 cells in iCko brain. Other YFP$^+$ cells in iCko cortex have the polydendrocyte morphology (arrow in A). All the YFP$^+$ cells in iCtr cortex (B) are Olig2$^+$ and GS$^-$ (arrows). Scale bars: 20 μm. (**C**) The proportion of astrocytes among Olig2-deleted progeny of NG2 cells. Data are the percentage of YFP$^+$ GS$^+$ Olig2$^-$ cells among all YFP$^+$ Olig2$^-$ cells in iCko cortex at 14 and 30 dpi. The values for iCtr cortex were 0% at both time points. Error bars indicate s.d.

In the neocortex of Olig2 Cko mice, NG2 cells appeared to be transforming from NG2 cells into astrocytes at P4 (Fig. 6). Several observations suggest that NG2 cells are converted into astrocytes postnatally and that EGFP$^+$ astrocytes do not arise from spurious EGFP expression in other sources of astrocytes such as radial glia. First, EGFP$^+$NG2$^+$ normal-appearing polydendrocytes exist in the neocortex at P0. Second, transitional forms suggestive of direct conversion of EGFP$^+$NG2$^+$ cells into EGFP$^+$ astrocytes were found at P4. These transitional cells co-expressed nuclear Sox10 and low levels of PDGFRα and NG2 in the distal processes along with Aldh1L1 immunoreactivity in the somata. We also observed clumps of NG2 immunoreactivity resembling ghosts of distal processes of NG2 cells (Fig. 2C), suggestive of residual NG2 that had not been completely degraded after transition from NG2 cells into astrocytes. Thus, Olig2 deletion causes disappearance of NG2 cells because Olig2-deleted NG2 cells downregulate polydendrocyte antigens and become astrocytes, and not because NG2 cells lacking Olig2 undergo cell death. Experiments using iCko mice further confirmed that NG2 cells initially appear in the perinatal neocortex and subsequently become astrocytes. In iCko mice, reporter$^+$ astrocytes appeared after Olig2 deletion was induced from P2 to P5, at an age when neocortical NG2 cells are already in place. However, the latency between Olig2 deletion and the appearance of NG2 cell-derived astrocytes increased with age. Despite loss of Olig2 immunoreactivity in 37% of YFP$^+$ cells one day after the last 4OHT injection at P5, the percentage of YFP$^+$ astrocytes gradually increased to 55% over 30 days. We previously reported the lack of transformation of NG2 cells into astrocytes when Olig2 was deleted in adult, even after stab wound injury (Komitova et al., 2011), consistent with other reports (Zawadzka et al., 2010; Rivers et al., 2008; Kang et al., 2010; Tripathi et al., 2010). These observations were extended only for 30 days, and it is possible that astrocytes are generated over a longer period of time after Olig2 deletion in NG2 cells in the mature brain.

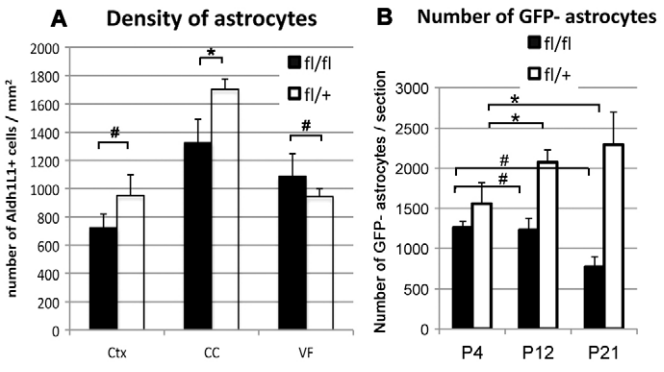

Fig. 8. Quantification of total astrocytes and resident astrocytes in Cko and Ctr brain. (**A**) There was no significant difference in astrocyte density in the neocortex (Ctx), corpus callosum (CC) or the ventral forebrain (VF). $^{\#}P>0.05$, $^{*}P=0.016$, one-way ANOVA with Tukey's post test. (**B**) The number of resident astrocytes per 50 μm section in the neocortex of Cko and Ctr mice at P4, P12 and P21. In Ctr neocortex, the number of EGFP$^-$ astrocytes increased with age (brackets, $^{*}P<0.05$). In Cko neocortex, the number of EGFP$^-$ astrocytes did not increase between P4 and P21 (brackets, $^{\#}P>0.05$). One-way ANOVA with Tukey's post-hoc test. Error bars indicate s.d.

Effects of Olig2 deletion on the fate of NG2 cells in different CNS regions

Different regions of the forebrain responded differently to Olig2 deletion in NG2 cells (Fig. 9). Curiously, the extent of astrocyte differentiation from NG2 cells was greater in the dorsal forebrain than in the ventral forebrain of Olig2 Cko mice, despite similar efficiencies of Olig2 deletion. The preservation of a greater number of NG2$^+$ cells in the ventral forebrain provides additional evidence for the lack of transformation of NG2 cells into astrocytes in the ventral forebrain, where NG2 cells normally contribute to one-third of the protoplasmic astrocyte population (Zhu et al., 2008a). Our findings are consistent with the dorsal ventral differences in myelin defects seen in mice in which Olig2 had been ablated in hGFAP$^+$ or the Emx-1$^+$ precursor cells (Yue et al., 2006). Olig2 may be playing a distinct role in fate determination of NG2 cells that arise from different sources described by Kessaris et al. (Kessaris et al., 2006). It is possible that a subpopulation of NG2 cells that arise from the Nkx2.1$^+$ and/or Gsx2$^+$ precursors in the medial and lateral ganglionic eminences spontaneously downregulate Olig2 and become astrocytes during normal embryonic development (Zhu et al., 2011), but those that remain NG2$^+$ are no longer dependent on Olig2 to remain in the oligodendrocyte lineage. In the dorsal forebrain, NG2 cells that arise from the Emx-1$^+$ precursor cells rarely generate astrocytes during normal development but can be reprogrammed to switch their fate to astrocytes upon artificial deletion of Olig2 (Fig. 9). Although NG2 cells generated from Gsx2 and Emx-1 domains appear to be functionally equivalent (Tripathi et al., 2011), there may be differences in their propensity to become astrocytes. Further studies are needed to determine

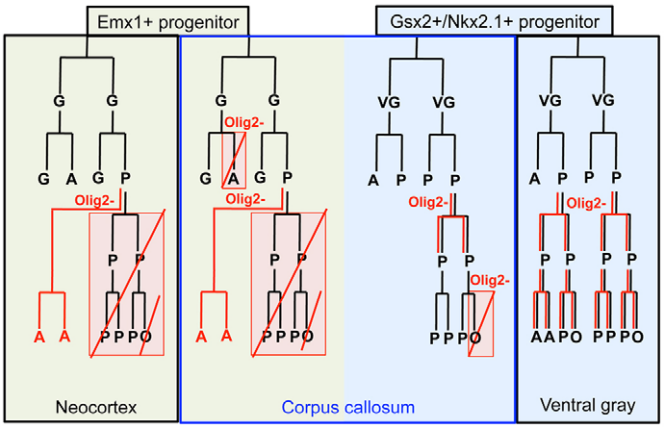

Fig. 9. Lineage diagram of NG2 cells in different forebrain regions. Proposed lineal relationship between polydendrocytes (NG2 cells), germinal cells, astrocytes and oligodendrocytes during normal development (black) and under Olig2-deleted conditions (red). Deletion of Olig2 converts the fate of NG2 cells from dorsal but not ventral origin into astrocytes, whereas ventral NG2 cells spontaneously generate astrocytes under normal conditions. Light green, lineage of dorsal cells; light blue, lineage of ventral cells; black box, gray matter; blue box, corpus callosum (which contains glial cells derived from both ventral and dorsal germinal cells); G, GFAP$^+$ dorsal germinal cell; VG, ventral germinal cell; A, astrocyte; P, polydendrocyte (=NG2 cell); O, oligodendrocyte. The neuronal lineage is omitted for simplicity.

whether the transcription factor code of origin influences the astrogliogenic fate of NG2 cells and the molecular mechanism through which this occurs.

Olig2 appears to have multiple roles in the white matter. Conditional ablation of Olig2 with hGFAP-cre led to a severe reduction in the number of astrocytes in the white matter, suggesting that Olig2 is required for the formation of white matter astrocytes from SVZ progenitor cells or radial glia (Cai et al., 2007; Marshall et al., 2005). Consistent with our previous observation that NG2 is not expressed on neural progenitor cells of the SVZ (Komitova et al., 2009), we did not see such a dramatic reduction in astrocyte density in the corpus callosum of Cko mice (Fig. 8). The observed phenotype could result from a combination of differential effects of Olig2 deletion on NG2 cells from different sources that co-exist in the corpus callosum (Tripathi et al., 2011), as summarized in the lineage diagram in Fig. 9. Some NG2 cells, probably those arising from the Emx-1$^+$ dorsal progenitor cells, are converted into astrocytes upon Olig2 deletion, whereas the fate of other NG2 cells, possibly those originating in ventral sources appear not to be affected by Olig2 deletion. However, the absence of Olig2 in NG2 cells in the corpus callosum that had not been converted into astrocytes severely compromised their ability to differentiate into oligodendrocytes (Fig. 9).

Competition between the NG2 cell-derived astrocytes and existing astrocytes in Cko mice

In normal development, astrocytes in the neocortex are generated from radial glia (Voigt, 1989; Gray and Sanes, 1992; Malatesta et al., 2000) or SVZ progenitor cells (Levison and Goldman, 1993; Zerlin et al., 2004; Ganat et al., 2006) but not from NG2 cells. In Olig2 Cko mice, more than 70% of neocortical astrocytes were generated from NG2 cells without significantly increasing the density of total astrocytes, which suggests that NG2 cell-derived astrocytes compete with existing astrocytes to maintain a constant final astrocyte density. This is supported by the observation that proliferation of existing EGFP$^-$ Aldh1L1$^+$ astrocytes was reduced by more than sevenfold in the neocortex of P4 Cko mice, where NG2 cells were in the process of transforming into astrocytes. Furthermore, the normal increase in the number of EGFP-negative existing (normal) astrocytes seen in the Ctr neocortex between P4 and P21 did not occur in the Cko neocortex. As astrocytes are known to occupy non-overlapping territories (Bushong et al., 2002), there may be a contact-dependent mechanism that regulates their density (Nakatsuji and Miller, 2001).

In summary, the findings described here indicate that NG2 cells in the embryonic and early postnatal brain exhibit developmental fate switch from oligodendrocytes to astrocytes in vivo upon removal of Olig2. Further studies are required to elucidate the molecular mechanism of Olig2-dependent fate switch that appears to be regulated in a region-specific manner.

Acknowledgements

We thank Drs Chuck Stiles and John Alberta (Dana-Faber Cancer Institute, Harvard Medical School, Boston, MA) for the Olig2 antibody, and Bill Stallcup (Burnham Institute, La Jolla, CA) for the NG2 antibodies. We thank Youfen Sun for her assistance in maintaining the mouse colony.

Funding

This work was supported by grants from the National Multiples Sclerosis Society [RG2826-B4 to A.N.], National Science Foundation and National Institutes of Health [R21 NS 069960 and R01 NS 073425 to A.N., K01 MH086050 to B.J.M., R01 NS 072427 and R01 NS 075243 to Q.R.L. and MH056524 to J.L.T.]. Deposited in PMC for release after 12 months.

Competing interests statement

The authors declare no competing financial interests.

Supplementary material

Supplementary material available online at
http://dev.biologists.org/lookup/suppl/doi:10.1242/dev.078873/-/DC1

References

Bushong, E. A., Martone, M. E., Jones, Y. Z. and Ellisman, M. H. (2002). Protoplasmic astrocytes in CA1 stratum radiatum occupy separate anatomical domains. *J. Neurosci.* **22**, 183-192.

Cahoy, J. D., Emery, B., Kaushal, A., Foo, L. C., Zamanian, J. L., Christopherson, K. S., Xing, Y., Lubischer, J. L., Krieg, P. A., Krupenko, S. A. et al. (2008). A transcriptome database for astrocytes, neurons, and oligodendrocytes: a new resource for understanding brain development and function. *J. Neurosci.* **28**, 264-278.

Cai, J., Chen, Y., Cai, W. H., Hurlock, E. C., Wu, H., Kernie, S. G., Parada, L. F. and Lu, Q. R. (2007). A crucial role for Olig2 in white matter astrocyte development. *Development* **134**, 1887-1899.

Dimou, L., Simon, C., Kirchhoff, F., Takebayashi, H. and Gotz, M. (2008). Progeny of Olig2-expressing progenitors in the gray and white matter of the adult mouse cerebral cortex. *J. Neurosci.* **28**, 10434-10442.

Fukuda, S., Kondo, T., Takebayashi, H. and Taga, T. (2004). Negative regulatory effect of an oligodendrocytic bHLH factor OLIG2 on the astrocytic differentiation pathway. *Cell Death Differ.* **11**, 196-202.

Ganat, Y. M., Silbereis, J., Cave, C., Ngu, H., Anderson, G. M., Ohkubo, Y., Ment, L. R. and Vaccarino, F. M. (2006). Early postnatal astroglial cells produce multilineage precursors and neural stem cells in vivo. *J. Neurosci.* **26**, 8609-8621.

Gray, G. E. and Sanes, J. R. (1992). Lineage of radial glia in the chicken optic tectum. *Development* **114**, 271-283.

Hack, M. A., Saghatelyan, A., de Chevigny, A., Pfeifer, A., Ashery-Padan, R., Lledo, P. M. and Gotz, M. (2005). Neuronal fate determinants of adult olfactory bulb neurogenesis. *Nat. Neurosci.* **8**, 865-872.

Jiao, Y., Sun, Z., Lee, T., Fusco, F. R., Kimble, T. D., Meade, C. A., Cuthbertson, S. and Reiner, A. (1999). A simple and sensitive antigen retrieval method for free-floating and slide-mounted tissue sections. *J. Neurosci. Methods* **93**, 149-162.

Kang, S. H., Fukaya, M., Yang, J. K., Rothstein, J. D. and Bergles, D. E. (2010). NG2+ CNS glial progenitors remain committed to the oligodendrocyte lineage in postnatal life and following neurodegeneration. *Neuron* **68**, 668-681.

Kessaris, N., Fogarty, M., Iannarelli, P., Grist, M., Wegner, M. and Richardson, W. D. (2006). Competing waves of oligodendrocytes in the

forebrain and postnatal elimination of an embryonic lineage. *Nat. Neurosci.* **9**, 173-179.
Kitada, M. and Rowitch, D. H. (2006). Transcription factor co-expression patterns indicate heterogeneity of oligodendroglial subpopulations in adult spinal cord. *Glia* **54**, 35-46.
Komitova, M., Zhu, X., Serwanski, D. R. and Nishiyama, A. (2009). NG2 cells are distinct from neurogenic cells in the postnatal mouse subventricular zone. *J. Comp. Neurol.* **512**, 702-716.
Komitova, M., Serwanski, D. R., Lu, Q. R. and Nishiyama, A. (2011). NG2 cells are not a major source of reactive astrocytes after neocortical stab wound injury. *Glia* **59**, 800-809.
Kondo, T. and Raff, M. (2004). Chromatin remodeling and histone modification in the conversion of oligodendrocyte precursors to neural stem cells. *Genes Dev.* **18**, 2963-2972.
Levine, J. M. and Stallcup, W. B. (1987). Plasticity of developing cerebellar cells *in vitro* studied with antibodies against the NG2 antigen. *J. Neurosci.* **7**, 2721-2731.
Levison, S. W. and Goldman, J. E. (1993). Both oligodendrocytes and astrocytes develop from progenitors in the subventricular zone of postnatal rat forebrain. *Neuron* **10**, 201-212.
Li, H., de Faria, J. P., Andrew, P., Nitarska, J., Richardson, W. D. (2011). Phosphorylation regulates OLIG2 cofactor choice and the motor neuron-oligodendrocyte fate switch. *Neuron* **69**, 918-929.
Ligon, K. L., Kesari, S., Kitada, M., Sun, T., Arnett, H. A., Alberta, J. A., Anderson, D. J., Stiles, C. D. and Rowitch, D. H. (2006). Development of NG2 neural progenitor cells requires Olig gene function. *Proc. Natl. Acad. Sci. USA* **103**, 7853-7858.
Lin, S. C. and Bergles, D. E. (2002). Physiological characteristics of NG2-expressing glial cells. *J. Neurocytol.* **31**, 537-549.
Lu, Q. R., Sun, T., Zhu, Z., Ma, N., Garcia, M., Stiles, C. D. and Rowitch, D. H. (2002). Common developmental requirement for Olig function indicates a motor neuron/oligodendrocyte connection. *Cell* **109**, 75-86.
Maire, C. L., Wegener, A., Kerninon, C. and Nait Oumesmar, B. (2010). Gain-of-function of Olig transcription factors enhances oligodendrogenesis and myelination. *Stem Cells* **28**, 1611-1622.
Malatesta, P., Hartfuss, E. and Gotz, M. (2000). Isolation of radial glial cells by fluorescent-activated cell sorting reveals a neuronal lineage. *Development* **127**, 5253-5263.
Marshall, C. A., Novitch, B. G. and Goldman, J. E. (2005). Olig2 directs astrocyte and oligodendrocyte formation in postnatal subventricular zone cells. *J. Neurosci.* **25**, 7289-7298.
Menn, B., Garcia-Verdugo, J. M., Yaschine, C., Gonzalez-Perez, O., Rowitch, D. and Alvarez-Buylla, A. (2006). Origin of oligodendrocytes in the subventricular zone of the adult brain. *J. Neurosci.* **26**, 7907-7918.
Muroyama, Y., Fujiwara, Y., Orkin, S. H. and Rowitch, D. H. (2005). Specification of astrocytes by bHLH protein SCL in a restricted region of the neural tube. *Nature* **438**, 360-363.
Nakatsuji, Y. and Miller, R. H. (2001). Density dependent modulation of cell cycle protein expression in astrocytes. *J. Neurosci. Res.* **66**, 487-496.
Nishiyama, A. (2007). Polydendrocytes: NG2 cells with many roles in development and repair of the CNS. *Neuroscientist* **13**, 62-76.
Nishiyama, A., Komitova, M., Suzuki, R. and Zhu, X. (2009). Polydendrocytes (NG2 cells): multifunctional cells with lineage plasticity. *Nat. Rev. Neurosci.* **10**, 9-22.
Novak, A., Guo, C., Yang, W., Nagy, A. and Lobe, C. G. (2000). Z/EG, a double reporter mouse line that expresses enhanced green fluorescent protein upon Cre-mediated excision. *Genesis* **28**, 147-155.
Platel, J. C., Gordon, V., Heintz, T. and Bordey, A. (2009). GFAP-GFP neural progenitors are antigenically homogeneous and anchored in their enclosed mosaic niche. *Glia* **57**, 66-78.
Pringle, N. P., Yu, W. P., Howell, M., Colvin, J. S., Ornitz, D. M. and Richardson, W. D. (2003). Fgfr3 expression by astrocytes and their precursors: evidence that astrocytes and oligodendrocytes originate in distinct neuroepithelial domains. *Development* **130**, 93-102.
Rivers, L. E., Young, K. M., Rizzi, M., Jamen, F., Psachoulia, K., Wade, A., Kessaris, N. and Richardson, W. D. (2008). PDGFRA/NG2 glia generate myelinating oligodendrocytes and piriform projection neurons in adult mice. *Nat. Neurosci.* **11**, 1392-1401.
Setoguchi, T. and Kondo, T. (2004). Nuclear export of OLIG2 in neural stem cells is essential for ciliary neurotrophic factor-induced astrocyte differentiation. *J. Cell Biol.* **166**, 963-968.
Srinivas, S., Watanabe, T., Lin, C. S., William, C. M., Tanabe, Y., Jessell, T. M. and Costantini, F. (2001). Cre reporter strains produced by targeted insertion of EYFP and ECFP into the ROSA26 locus. *BMC Dev. Biol.* **1**, 4.
Stallcup, W. B. and Beasley, L. (1987). Bipotential glial precursor cells of the optic nerve express the NG2 proteoglycan. *J. Neurosci.* **7**, 2737-2744.
Steinhauser, C., Jabs, R. and Kettenmann, H. (1994). Properties of GABA and glutamate responses in identified glial cells of the mouse hippocampal slice. *Hippocampus* **4**, 19-35.
Takebayashi, H., Yoshida, S., Sugimori, M., Kosako, H., Kominami, R., Nakafuku, M. and Nabeshima, Y. (2000). Dynamic expression of basic helix-loop-helix Olig family members: implication of Olig2 in neuron and oligodendrocyte differentiation and identification of a new member, Olig3. *Mech. Dev.* **99**, 143-148.
Takebayashi, H., Nabeshima, Y., Yoshida, S., Chisaka, O. and Ikenaka, K. (2002). The basic helix-loop-helix factor olig2 is essential for the development of motoneuron and oligodendrocyte lineages. *Curr. Biol.* **12**, 1157-1163.
Tripathi, R. B., Rivers, L. E., Young, K. M., Jamen, F. and Richardson, W. D. (2010). NG2 glia generate new oligodendrocytes but few astrocytes in a murine experimental autoimmune encephalomyelitis model of demyelinating disease. *J. Neurosci.* **30**, 16383-16390.
Tripathi, R. B., Clarke, L. E., Burzomato, V., Kessaris, N., Anderson, P. N., Attwell, D. and Richardson, W. D. (2011). Dorsally and ventrally derived oligodendrocytes have similar electrical properties but myelinate preferred tracts. *J. Neurosci.* **31**, 6809-6819.
Voigt, T. (1989). Development of glial cells in the cerebral wall of ferrets: direct tracing of their transformation from radial glia into astrocytes. *J. Comp. Neurol.* **289**, 74-88.
Yue, T., Xian, K., Hurlock, E., Xin, M., Kernie, S. G., Parada, L. F. and Lu, Q. R. (2006). A critical role for dorsal progenitors in cortical myelination. *J. Neurosci.* **26**, 1275-1280.
Zawadzka, M., Rivers, L. E., Fancy, S. P., Zhao, C., Tripathi, R., Jamen, F., Young, K., Goncharevich, A., Pohl, H., Rizzi, M. et al. (2010). CNS-resident glial progenitor/stem cells produce Schwann cells as well as oligodendrocytes during repair of CNS demyelination. *Cell Stem Cell* **6**, 578-590.
Zerlin, M., Milosevic, A. and Goldman, J. E. (2004). Glial progenitors of the neonatal subventricular zone differentiate asynchronously, leading to spatial dispersion of glial clones and to the persistence of immature glia in the adult mammalian CNS. *Dev. Biol.* **270**, 200-213.
Zhou, Q. and Anderson, D. J. (2002). The bHLH transcription factors OLIG2 and OLIG1 couple neuronal and glial subtype specification. *Cell* **109**, 61-73.
Zhou, M., Schools, G. P. and Kimelberg, H. K. (2006). Development of GLAST(+) astrocytes and NG2(+) glia in rat hippocampus CA1: mature astrocytes are electrophysiologically passive. *J. Neurophysiol.* **95**, 134-143.
Zhu, X., Bergles, D. E. and Nishiyama, A. (2008a). NG2 cells generate both oligodendrocytes and gray matter astrocytes. *Development* **135**, 145-157.
Zhu, X., Hill, R. A. and Nishiyama, A. (2008b). NG2 cells generate oligodendrocytes and gray matter astrocytes in the spinal cord. *Neuron Glia Biol.* **4**, 19-26.
Zhu, X., Hill, R. A., Dietrich, D., Komitova, M., Suzuki, R. and Nishiyama, A. (2011). Age-dependent fate and lineage restriction of single NG2 cells. *Development* **138**, 745-753.

Table S1. Source and dilution of primary antibodies

Antibody	Host	Source	Dilution
Aldh1L1 (aldehyde dehydrogenase 1 L1)	mouse	NeuroMab (UC Davis, CA)	1:500
CC1	mouse	Oncogene	1:200
GFP	rabbit	Chemicon	1:500
GFP	mouse	Chemicon	1:500
GFP	chicken	Aves Labs	1:1000
GS (glutamine synthetase)	mouse	Millipore	1:1000
GST-π (glutathione S-transferase-π)	rabbit	MBL International	1:200
Ki-67	rabbit	Novacastra	1:200
MBP (myelin basic protein)	mouse	Sternberger Monoclonals	1:1000
NeuN	mouse	Chemicon	1:200
NG2	rabbit	Chemicon	1:500
NG2	guinea pig	Dr Stallcup*	1:200
Olig21	rabbit	Drs Stiles and Alberta‡	1:50,000
Olig2	rabbit	Abcam	1:500
PDGFRα	rabbit	Dr. Stallcup	1:1000
Sox10	rabbit	Chemicon	1:200
S100β	mouse	Sigma	1:2000

*Dr. William Stallcup, Burnham Institute, La Jolla, CA, USA.

‡Drs Charles Stiles and John Alberta, Dana-Farber Cancer Institute, Boston, MA, USA.